Influence of neutron transfer channels and collective excitations in the fusion of ^{28}Si with ^{90,92,94,96}Zr targets

Manjeet Singh Gautam [1,*] Sukhvinder Duhan,[2] Rishi Pal Chahal,[3] Hitender Khatri,[4] Suman B. Kuhar,[5] and K. Vinod[6]

[1]*Department of Physics, Government College Alewa, Jind, Haryana-126102, India*

[2]*Department of Applied Sciences and Humanities, Seth Jai Parkash Mukand Lal Institute of Engineering and Technology, Radaur, Yamunanagar, Haryana-135133, India*

[3]*Department of Physics, Chaudhary Bansi Lal University, Bhiwani, Haryana-127021, India*

[4]*Department of Physics, Pt. Neki Ram Sharma Government College, Rohtak, Haryana-124001, India*

[5]*Department of Physics, IHL, BPS Mahila Vishwavidyalaya, Khanpur Kalan Sonipat, Haryana-131305, India*

[6]*Department of Physics, Indus Degree College, Kinana, Jind, Haryana-126102, India*

(Received 30 March 2020; accepted 24 June 2020; published 17 July 2020)

This work theoretically explores the role of neutron transfer channels and/or collective inelastic surface excitations in the fusion of ^{28}Si with ^{90,92,94,96}Zr targets by using the coupled channel theory and the energy dependent Woods-Saxon potential (EDWSP) model. The series of ^{90,92,94,96}Zr targets is quite interesting due to the fact that the possibilities of neutron transfer channels with positive ground state Q values increase with the increase of isotopic mass. For ^{28}Si + ^{90}Zr reaction, the influences of inelastic surface excitations turned out to be important and coupling of such channels to their relative motion reproduced the experimental data. In the case of ^{28}Si + ^{92}Zr reaction, in addition to consideration of low lying states such as 2^+ and 3^- vibrational states of colliding nuclei, the coupling to two neutron pickup channels is necessarily required to address the sub-barrier fusion anomalies. For ^{28}Si + ^{94,96}Zr reactions, the inclusions of multiphonon states of type 2^+ and 3^- of colliding nuclei were not able to reproduce the fusion enhancement particularly at below barrier energies. In this case, neutron transfer channels with positive ground state Q value play a crucial role in the enhancement of fusion cross-section data at sub-barrier energies and therefore must be included in the coupled channel description. In distinction, in the EDWSP model, the energy dependence in the nucleus-nucleus potential causes barrier modification effects and subsequently induces a barrier lowering phenomenon. In this way, the EDWSP based outcomes reasonably address the sub-barrier fusion anomalies of ^{28}Si + ^{90,92,94,96}Zr reactions and thus impacts of dominant intrinsic channels are intrinsically included due to the dynamical nature of the energy dependent interaction potential. For studied systems, the EDWSP outcomes are able to achieve an agreement with the portion of above barrier fusion data within 10% with a probability greater than 90%. Within this model, 33 fusion data points out of 38 fusion data points lie within 5%. Only five fusion data points lie within 10% and thereby the EDWSP model adequately addresses the fusion anomalies of the chosen reactions. The smaller values of χ^2 analysis for the EDWSP calculations, which range from 2.82 to 3.14, indicate that the model predictions appropriately describe the observed fusion dynamics of the studied reactions.

DOI: 10.1103/PhysRevC.102.014614

I. INTRODUCTION

Heavy ion fusion reactions with many degrees of freedom are examples of multidimensional quantum tunneling and have been the subject of theoretical and experimental interest during the past few decades [1–4]. It was believed that the fusion of two nuclei could be understood in terms of the one-dimensional barrier penetration model (BPM), wherein the relative motion between the collision partners is the only degree of freedom. According to one-dimensional BPM, the projectile and target nuclei have to penetrate the Coulomb barrier between them and subsequently form the compound nucleus. However, the experimentally observed fusion cross-section data turned out to be significantly larger than the expectations of the one-dimensional BPM [5–8]. In the literature, to reproduce the observed fusion excitation function data, the coupling of nuclear structure degrees of freedom like collective surface excitations, zero point motion of nuclear surface, neck formation, static deformation, and higher order deformation, rotations of participating nuclei during nuclear collision and/or nucleon transfer channels to their relative motion have been considered within the context of the various theoretical approaches [9–12]. Various authors [13–23] suggested that the influences of the low lying vibrational states associated with the fusing pairs, permanent shape deformation, and higher order deformation of a projectile (or target) in its ground state and/or nucleon transfer channels are found to be important in the substantially large enhancement of fusion cross sections particularly at below barrier

*gautammanjeet@gmail.com

energies. The understanding of the role of the surface vibrational couplings and rotational couplings on the fusion process has been achieved partially but many aspects in this direction are still unexplored [24–37]. On the other hand, the dynamics of neutron transfer is more complex due to the fact that neutron transfer offers no barrier during the nuclear interactions and seems to participate actively at much larger internuclear separation between collision partners and hence enhances the magnitude of fusion cross section at near and sub-barrier energies [38–51]. Zagrebaev [52], has developed a semiclassical approach to handle the nucleon transfer channels with positive ground state Q values in an approximate way. Using this model, the author obtained good fits to the fusion dynamics of ^{40,48}Ca + ^{48}Ca, ^{48}Ca + ^{90,96}Zr, ^{18}O + ^{58}Ni, and ^{16}O + ^{60}Ni reactions and claimed that transfer with negative Q values has no effect on fusion enhancement at near and below-barrier energies. In other words, the sub-barrier fusion enhancement is quite insensitive to neutron transfer channels with negative ground state Q values. Sargsyan and co-workers [53,54], using a quantum diffusion approach, suggested that neutron transfer channels weakly affect the fusion dynamics if the deformation strength of the participant nuclei does not change or decrease after neutron transfer. Therefore, in some cases despite neutron transfer with positive Q value, the strong sub-barrier fusion enhancements due to transfer channels were not observed. Zhang *et al.* [55], systematically analyzed the effects of positive Q-value neutron transfer channels on the fusion process for many fusing systems and using a universal fusion functions approach arrived at the aforementioned conclusions. The authors concluded that after neutron transfer if deformation of participating nuclei increases by a large amount then there is strong sub-barrier fusion enhancement, which occurs as a consequence of the positive Q-value neutron transfer channels. On the other hand, if the deformation of interacting nuclei is small or almost unchanged or decreases after neutron transfer, the fusion cross sections remain almost unaffected due to positive Q-value neutron transfer channels. In this regard, the role of neutron transfer channels is seemingly elusive in many cases, which in turn, makes fusion dynamics puzzling. Many features of such reactions have not yet been understood fully and hence it is an open area to explore the influences of rearrangements of nucleons along with the nuclear structure of fusing pairs on theoretical as well as on experimental grounds.

The systematic studies involving common projectile (or target) usually are more informative than those of the individual case. In general, projectile-target combinations, wherein one of the reaction partners has a closed shell or closed subshell, provides a better platform in the understanding of the fusion dynamics in the domain of the Coulomb barrier. In this direction, some authors carried out their pioneering work [1–3,8–13,56–58] and tried to understand anomalies of various heavy ion fusion reactions but still success has been achieved partially. The fusion mechanism involving the bombardment of different projectiles on a series of Zr targets represents a benchmark due to the fact that as one moves from a lighter target (^{90}Zr) to a heavier one (^{96}Zr), the target becomes more and more soft and offers possibilities of nucleon transfer channels [17,21,22,39–44]. With the increase of neutron richness in a target, the strength of octupole vibrations almost increases and the corresponding excitation energy decreases, henceforth, influences of the vibrational couplings on the fusion process are expected to increase with the increase of isotopic mass in the target. As a Zr isotope with $Z = 40$ has proton subshell closure, the proton transfer channels are not expected to have special significance in the fusion process. A ^{90}Zr nucleus has a neutron closed shell and in ^{92,94,96}Zr isotopes, neutrons lie outside of neutron closed shell and hence facilitate neutron transfer with positive Q value during the fusion process. The fusion of ^{28}Si with ^{90,92,94,96}Zr targets have been experimentally investigated [59–63], wherein authors tried to extricate the significance of the transfer coupling from the collective excitations associated with the colliding pairs.

For ^{28}Si + ^{92}Zr reaction, Newton *et al.* [59] used a beam of ^{28}Si in the energy range ($E_{\rm lab}$) of 86–107 MeV on a ^{92}Zr target and precisely measured the fusion cross-section data using ANU 14UD Pelletron accelerator in Australia. Authors using the coupled channel approach analyzed the experimental data of ^{28}Si + ^{92}Zr reaction and pointed out that fusion data are quite sensitive to the collective excitations associated with the collision partners as well as the neutron transfer channels with positive ground state Q value. For this reaction, 2n-pickup channel with Q value equal to +3.25 MeV exists, which in turn significantly affects the fusion yields. Such channel must be incorporated in the coupled channel description in order to gain reasonable agreement with the experimentally observed data. For ^{28}Si + ^{90,94}Zr reactions [60], Kalkal *et al.* carried out measurements for fusion cross-section data in the energy range ($E_{\rm lab}$) of 82–120 MeV by using a pulsed ^{28}Si beam from the 15UD Pelletron accelerator at the Inter-University Accelerator Centre (IUAC), New Delhi, India. Experimentally, a pulsed ^{28}Si beam was incident on ^{90,94}Zr targets for observing the complete fusion events. Theoretically, the fusion enhancement of the ^{28}Si + ^{90}Zr reaction relative to one dimensional BPM was explained by incorporating the low lying inelastic states of the fusing pairs, while in the case of the ^{28}Si + ^{94}Zr reaction, the fusion enhancements at sub-barrier energies could not be reproduced by considering the inelastic surface excitations alone and thus one has to include the multineutron transfer channels with positive ground state Q value in the coupled channel analysis. Kalkal *et al.* [61,62], using the heavy ion reaction analyzer (HIRA) at IUAC, New Delhi, India, also measured experimental data for the multinucleon transfer channels like one and two proton transfer, and one neutron and two neutron pickup channels. The authors have highlighted the influences of these channels on the fusion process. Khushboo *et al.* [63] have used a pulsed beam of ^{28}Si from the 15UD Pelletron accelerator at the Inter-University Accelerator Centre (IUAC), New Delhi, India in the energy range ($E_{\rm lab}$) of 81.4–119.5 MeV on ^{92,96}Zr targets and measured the fusion cross-section data for ^{28}Si + ^{92,96}Zr reactions. For the ^{28}Si + ^{96}Zr reaction, in addition to the collective inelastic surface excitations, the couplings to multineutron transfer channels with the positive ground state Q values are needed to adequately address the fusion enhancements, particularly at below barrier energies. For ^{28}Si + ^{94,96}Zr reactions, the considerations of multiphonon states of type 2^+

and 3^- in the coupled channel analysis are unable to provide an appropriate description of the experimental data. In this way, the fusion dynamics of ^{28}Si + ^{90,92,94,96}Zr reactions unambiguously reveal the role of multineutron transfer channels and/or low lying collective vibrational states and henceforth attracts researchers to explore them by using different theoretical approaches.

Keeping in mind the aforementioned issues, this work analyzes the fusion dynamics of ^{28}Si + ^{90,92,94,96}Zr reactions within the framework of the coupled channel method [64] and the energy dependent Woods-Saxon potential (EDWSP) model [65–68]. The coupled channel calculations are performed by using the code CCFULL, wherein couplings to all orders have been included. From the present coupled channel analysis, one can easily point out the influences of the inelastic surface excitations and/or multineutron transfer channels with positive ground state Q values on the fusion process. In order to extract more concrete conclusions regarding neutron transfer couplings, the fusion mechanisms of ^{28}Si + ^{90,92,94,96}Zr reactions have been investigated by using the energy dependent interaction potential [65–68]. Very recently [69–73], the EDWSP model has been successfully utilized for an adequate description of the fusion dynamics of the stable and weakly bound nuclei and hence is an efficient theoretical tool for exploring the role of collective vibrational states and/or nucleon transfer channels on fusion process. In EDWSP calculations, the range parameter increases with the increase of neutron richness in a target, which clarified that greater barrier modifications are needed to explain the experimental data of ^{28}Si + ^{90,92,94,96}Zr reactions. The increasing trend of range parameter, which reflects the dominance of collective excitations and/or neutron transfer channels, is also consistent with the nuclear structure of the target isotopes. In the present model, the energy dependence in the nucleus-nucleus potential generates the barrier lowering effects and thereby predicts larger sub-barrier fusion cross sections in comparison to the outcomes of the one dimensional BPM. In this way, the EDWSP based results reasonably explain the fusion mechanism of the given reactions under consideration. A brief description of the theoretical formalism is given in Sec. II. The results of calculations are given in detail in Sec. III and the conclusions drawn are discussed in Sec. IV.

II. THEORETICAL FORMALISM

A. Energy dependent Woods-Saxon Potential (EDWSP) model

The total fusion cross section using the partial wave analysis is defined as

$$\sigma_F = \frac{\pi}{k^2}\sum_{\ell=0}^{\infty}(2\ell+1)T_\ell^F, \tag{2.1}$$

where, $k^2 = \frac{2\mu E_{\rm c.m.}}{\hbar^2}$, μ is the reduced mass of colliding nuclei, and $E_{\rm c.m.}$ is the incident energy of relative motion in the center of mass frame. Based on the parabolic approximation, Hill and Wheeler proposed an expression for tunneling probability (T_ℓ^F), wherein the effective interaction between the collision partners is replaced by an inverted parabola [74],

$$T_\ell^{\rm HW} = \frac{1}{1+\exp\left[\frac{2\pi}{\hbar\omega_\ell}(V_\ell - E_{\rm c.m.})\right]}, \tag{2.2}$$

where $\hbar\omega_\ell$ and V_ℓ are the barrier curvature and barrier height for ℓth partial wave respectively. Within the parabolic approximation, the tunneling probability T_ℓ^F in Eq. (2.1) is replaced by $T_\ell^{\rm HW}$ and thus results in the following expression for the fusion cross sections:

$$\sigma_F = \frac{\pi}{k^2}\sum_{\ell=0}^{\infty}(2\ell+1)\frac{1}{1+\exp\left[\frac{2\pi}{\hbar\omega_\ell}(V_\ell - E_{\rm c.m.})\right]}. \tag{2.3}$$

This approximation was further simplified by Wong [75]. Wong makes the use of the following approximations for barrier position R_B, barrier height V_{B0}, and barrier curvature $\hbar\omega$:

$$R_\ell = R_{\ell=0} = R_B, \tag{2.4}$$

$$\omega_\ell = \omega_{\ell=0} = \omega, \tag{2.5}$$

$$V_\ell = V_{B0} + \frac{\hbar^2}{2\mu R_B^2}\left[\ell+\frac{1}{2}\right]^2. \tag{2.6}$$

Using Eqs. (2.4)–(2.6) into Eq. (2.3) and by taking the effects of the infinite number of partial waves for the fusion process, Wong obtained the following expression for estimating the fusion cross section. This formula is known as the one dimensional Wong formula [75]:

$$\sigma_F = \frac{\hbar\omega R_B^2}{2E_{\rm c.m.}}\ell n\left[1+\exp\left(\frac{2\pi}{\hbar\omega}(E_{\rm c.m.}-V_{B0})\right)\right], \tag{2.7}$$

wherein R_B, V_{B0}, and $\hbar\omega$ are barrier position, barrier height, and barrier curvature respectively for the Coulomb barrier. In the EDWSP model [65–73], the energy dependent interaction potential has been used along with the one dimensional Wong formula [75]. Very recently, the fusion of spherical nuclei, wherein either nucleon (or multinucleon) transfer channels or collective surface vibrational modes or both are important modes of couplings, was successfully analyzed by considering the EDWSP model. In this model, the form of nuclear potential is taken to be of the Woods-Saxon type and is defined as

$$V_N(r) = \frac{-V_0}{\left[1+\exp\left(\frac{r-R_0}{a}\right)\right]} \tag{2.8}$$

with $R_0 = r_0(A_P^{1/3} + A_T^{1/3})$. The quantity "$V_0$" is the depth and "$a$" is the diffuseness parameter of the Woods-Saxon potential. In the present case, the Coulomb potential between fusing systems is described as

$$V_C(r) = \frac{Z_P Z_T e^2}{r} \tag{2.9}$$

with, $Z_P(Z_T)$ the charge on the projectile (target) nucleus. In the EDWSP model, the depth parameter (V_0) is defined

as

$$V_0 = \left[A_P^{2/3} + A_T^{2/3} - (A_P + A_T)^{2/3}\right] \times \left[2.38 + 6.8(1 + I_P + I_T)\frac{A_P^{1/3}A_T^{1/3}}{\left(A_P^{1/3} + A_T^{1/3}\right)}\right] \text{ MeV}, \tag{2.10}$$

where $I_P = (\frac{N_P - Z_P}{A_P})$ and $I_T = (\frac{N_T - Z_T}{A_T})$ are the isospin asymmetry of projectile and target respectively. The EDWSP model includes the effects of surface energy as well as the isospin asymmetry of colliding pairs. The above parametrization of potential depth is based upon the reproduction of the fusion excitation function data of various projectile-target combinations ranging $Z_P Z_T = 84$ to $Z_P Z_T = 1640$. The various static and dynamical physical effects during the fusion process occur in the surface region of nuclear potential or in the tail region of the Coulomb barrier. These physical effects are responsible for modification of potential parameters. The first term in the square bracket of Eq. (2.10) is directly proportional to surface energy of the colliding nuclei and hence strongly depends on the collective motion of all nucleons inside the nucleus. The various channel coupling effects, which are responsible for large fusion enhancement at sub-barrier energies, are the surfacial effects. Such surfacial effects produce fluctuation in the surface diffuseness as well as the surface energy of the collision partners during the fusion process. At very short distances, the overlap density exceeds the saturation density of the colliding nuclei and is a dynamical density evolution wherein surface diffuseness and surface energy are strongly affected. Furthermore, the other dynamical effects such as variations of N/Z ratio, dissipation of kinetic energy of relative motion to nuclear structure degrees of freedom of the collision partners, and variations of densities (dynamical density evolutions) of collision partners in the neck region also fluctuate the diffuseness parameter and hence bring the necessity of larger diffuseness ranging from $a = 0.75$ fm to $a = 1.5$ fm for reproduction of fusion excitation function data [8–13,76,77]. This anomaly in the diffuseness parameter is known as the diffuseness anomaly and the cause of the diffuseness anomaly is still unknown. The abnormally large value of diffuseness parameter is an artifact masking of various dynamical effects and hence is responsible for the systematic failure of the static Woods-Saxon potential for simultaneously accounting of the elastic scattering data and fusion data. The surface region of the nuclear potential is more sensitive to small changes in nucleon density parameters than the inner region. The nuclear structure effects of the participant nuclei, which are mostly present at the surface region, are mainly related to the diffuseness parameter of the nuclear potential. In this sense, due to nuclear structure effects, the strengths of nuclear potential may vary significantly at the surface regions, which can be accommodated just by optimizing the diffuseness parameter of the nuclear potential. The second term inside the square bracket of Eq. (2.10) is directly related to isospin asymmetry effects of colliding nuclei which is different for different isotopes of a particular element. The isotopic effects of reactants enter in the nucleus-nucleus potential via this term. In the fusion process, the present prescription of potential depth includes the effects of variations of surface energy as well as the isospin asymmetry of the colliding nuclei.

In addition to aforementioned physical effects, the energy dependence in the nucleus-nucleus potential also originates from nonlocal quantum effects [78–82]. In a recent analysis, it has been explicitly shown that as a consequence of the channel coupling effects, the nucleus-nucleus potential becomes energy dependent in the domain of the Coulomb barrier [78–85]. Therefore, all such relevant physical effects are included in the present model by considering the energy dependence in the Woods-Saxon potential via its diffuseness parameter. In the EDWSP model, the energy dependent diffuseness parameter is described as

$$a(E) = 0.85\left[1 + \frac{r_0}{13.75\left(A_P^{-1/3} + A_T^{-1/3}\right)\left[1 + \exp\left(\frac{\frac{E}{V_{B0}} - 0.96}{0.03}\right)\right]}\right] \text{ fm}. \tag{2.11}$$

In order to obtain this expression, we have reproduced the fusion excitation function data by varying the diffuseness parameter of the Woods-Saxon nuclear potential for a wide range of projectile and target combinations and the sigmoidal fitting leads to the above expression. In Eq. (2.11), the range parameter (r_0) is adjusted in order to compensate for the dominant channel coupling effects for a given reaction under study. The range parameter strongly depends on the nature of the colliding system as well as on the nature of dominant nuclear structure degrees of freedom like collective excitations, static deformation, nucleon (multinucleon) transfer channels, and other static and dynamical physical effects. As three potential parameters (r_0, a, and V_0) are intrinsically linked with each other, consequently any variation in one parameter automatically brings corresponding modifications in the other parameters. In our formalism, V_0 depends on the surface energy as well as the isospin term of the reacting pairs [see Eq. (2.10)] while the other two parameters (r_0 and a) are interrelated through Eq. (2.11). The change in diffuseness directly depends on the range parameter (r_0) that is further related to the geometrical structure of fusing systems via the relation $R_0 = r_0(A_P^{1/3} + A_T^{1/3})$. This radius parameter is also defined in the various coupled channel formalisms, which are generally used to describe heavy ion fusion reactions. The impacts of the intrinsic degrees of freedom of the colliding pairs and other static and dynamical physical effects are incorporated through this radius parameter [1–3,8–13,56–58,86]. The range parameters used in the EDWSP calculations are consistent with the commonly adopted values ($r_0 = 0.90$ fm to $r_0 = 1.35$ fm), which are generally employed in the

literature within the context of the different theoretical approaches for different reactions [1–3,8–13,56–58,86].

B. Coupled channel model

In this section, a brief outline of the coupled channel approach used for theoretical calculations of the fusion excitation function is presented. In the coupled channel method, the internal structure degrees of freedom of the fusing partners such as collective excitations, permanent shape deformation, and/or nucleon (multinucleon) transfer channels that are generally coupled with their relative motion have been entertained. In this method, the following sets of coupled channel equations [64,87–89] are to be solved numerically:

$$\left[\frac{-\hbar^2}{2\mu}\frac{d^2}{dr^2}+\frac{J(J+1)\hbar^2}{2\mu r^2}+V_N(r)+\frac{Z_P Z_T e^2}{r}+\varepsilon_n-E_{c.m.}\right]\psi_n(r) + \sum_m V_{nm}(r)\psi_m(r)=0. \tag{2.12}$$

where $\vec{r}$ is the radial coordinate for the relative motion between the fusing nuclei. μ is defined as the reduced mass of the projectile and target system. $E_{\text{c.m.}}$ and ε_n are the bombarding energy in the center of mass frame and the excitation energy of the nth channel respectively. V_{nm} is the matrix elements of the coupling Hamiltonian, which in the collective model consists of the Coulomb and nuclear parts. The coupled channel calculations are performed by using the code CCFULL [64], wherein the coupled channel equations are solved numerically. This code includes the couplings to all orders. The sets of coupled channel equations are solved by imposing the isocentrifugal approximation and ingoing wave boundary conditions (IWBCs). In the isocentrifugal approximation, one can replace the total angular momentum of the relative motion of each channel by the total angular momentum. This code also undertakes the effects of finite excitation energy of the intrinsic motion [64,87–89]. The ingoing wave boundary conditions (IWBCs), which are well applicable for heavy ion reactions, are used to obtain the numerical solution of the coupled differential equations [64,87–89]. By including the dominant effects of the nuclear structure degrees of freedom, the total fusion cross section can be written as

$$\sigma_F(E_{\text{c.m.}})=\sum_J \sigma_J(E_{\text{c.m.}})=\frac{\pi}{k_0^2}\sum_J (2J+1)P_J(E_{\text{c.m.}}), \tag{2.13}$$

where $P_J(E_{\text{c.m.}})$ is the total transmission coefficient corresponding to the angular momentum J. In the code CCFULL, the rotational coupling with a pure rotor and a vibrational coupling in the harmonic limit are taken into account. The operator in the nuclear coupling Hamiltonian for rotational and vibrational couplings respectively is given by

$$\hat{O}_R=\beta_2 R_T Y_{20}+\beta_4 R_T Y_{40} \tag{2.14}$$

and

$$\hat{O}_V=\frac{\beta_\lambda}{\sqrt{4\pi}}R_T(a^\dagger_{\lambda 0}+a_{\lambda 0}). \tag{2.15}$$

Above R_T is parametrized as $r_{\text{coup}}A^{1/3}$, β_λ is the deformation parameters, and $a^\dagger_{\lambda 0}$ ($a_{\lambda 0}$) is the creation (annihilation) operator of the phonon of vibrational mode of multipolarity λ. In general, the nuclear coupling matrix elements are evaluated as

$$V^{(N)}_{nm}=\langle n|V_N(r,\hat{O})|m\rangle - V^{(0)}_N\delta_{n,m}. \tag{2.16}$$

For rotational couplings, the matrix elements of $\hat{O}_R$ between the $|n\rangle=|I0\rangle$ and $|m\rangle=|I'0\rangle$ states of the rotational band and the matrix elements of the $\hat{O}_V$ between the n-phonon state $|n\rangle$ and the m-phonon state $|m\rangle$ are needed for vibrational coupling, which are given by

$$\hat{O}_{R(I,I')}=\sqrt{\frac{5(2I+1)(2I'+1)}{4\pi}}\beta_2 R_T\begin{pmatrix} I & 2 & I' \\ 0 & 0 & 0\end{pmatrix}^2 + \sqrt{\frac{9(2I+1)(2I'+1)}{4\pi}}\beta_4 R_T\begin{pmatrix} I & 4 & I' \\ 0 & 0 & 0\end{pmatrix}^2 \tag{2.17}$$

and

$$\hat{O}_{V(nm)}=\frac{\beta_\lambda}{\sqrt{4\pi}}R_T(\delta_{n,m-1}\sqrt{m}+\delta_{n,m+1}\sqrt{n}), \tag{2.18}$$

respectively. The Coulomb coupling matrix elements are computed by linear coupling approximation and are given by

$$V^{(C)}_{R(I,I')}=\frac{3Z_P Z_T R_T^2}{5r^3}\sqrt{\frac{5(2I+1)(2I'+1)}{4\pi}}\left(\beta_2+\frac{2}{7}\beta_2^2\sqrt{\frac{5}{\pi}}\right)\begin{pmatrix} I & 2 & I' \\ 0 & 0 & 0\end{pmatrix}^2 + \frac{3Z_P Z_T R_T^4}{9r^5}\sqrt{\frac{9(2I+1)(2I'+1)}{4\pi}}\left(\beta_4+\frac{9}{7}\beta_2^2\right)\begin{pmatrix} I & 4 & I' \\ 0 & 0 & 0\end{pmatrix}^2 \tag{2.19}$$

and

$$V^{(C)}_{V(nm)}=\frac{\beta_\lambda}{\sqrt{4\pi}}\frac{3}{2\lambda+1}Z_P Z_T e^2\frac{R_T^\lambda}{r^{\lambda+1}}(\sqrt{m}\delta_{n,m-1}+\sqrt{n}\delta_{n,m+1}) \tag{2.20}$$

for the rotational and vibrational couplings respectively. The total coupling matrix elements are obtained by taking the sum of $V^{(N)}_{nm}$ and $V^{(C)}_{nm}$. In the code CCFULL, the effects of a pair transfer coupling between the ground states have been

TABLE I. The deformation parameter (β_λ) and the excitation energy (E_λ) of the quadrupole and octupole vibrational states along with the spins and parties for the various nuclei.

Nucleus	β_2	E_2(MeV)	β_3	E_3(MeV)	Reference
^{28}Si	−0.407	1.780	0.280	6.880	[59]
^{90}Zr	0.090	2.186	0.220	2.748	[41]
^{92}Zr	0.100	0.934	0.170	2.340	[41]
^{94}Zr	0.090	0.919	0.200	2.058	[41]
^{96}Zr	0.080	1.751	0.270	1.897	[41]

included. The microscopic coupling form factor for transfer channels is defined as

$$F_{\text{Trans}}(r) = F_t \frac{dV_N}{dr} \tag{2.21}$$

with F_t the coupling strength, which can be varied in order to gain optimum fit with the experimental data.

III. RESULTS AND DISCUSSION

The deformation parameter and their corresponding excitation energy of low lying 2^+ and 3^- vibrational states of projectile and targets are listed in Table I. The barrier height, barrier position, and barrier curvature for colliding, which are used in the EDWSP calculations, are listed in Table II. In Table III, the potential parameters such as range, depth, and diffuseness that are used in the coupled channel calculations for the studied reactions are listed. In Table IV, the parameters of the EDWSP model, such as range, depth, and diffuseness, used in the calculations, are listed. The Q values for nucleon (multinucleon) transfer channels are given in Tables V and VI.

A. Coupled channel analysis

For ^{28}Si + ^{90}Zr reaction, the coupled channel calculations, as done by using the code CCFULL [64], are shown in Fig. 1(a). In the no-coupling description, the projectile and target are taken as inert, wherein the relative motion between the collision partners is the only degrees of freedom. The no-coupling results are substantially smaller than that of the fusion data in near and below barrier energy regions. As already mentioned, the target is the spherical nucleus and the low lying states such as 2^+ and 3^- vibrational states seem to be very important. The effects of coupling of the 3^- vibrational state of target are found to be much larger than that of the 2^+ vibrational state, which clearly intimates that the 3^- vibrational state is more effective than that of the 2^+ vibrational state. The one phonon 2^+ and 3^- vibrational states of target are coupled to relative motion and their influences are considered in the coupled channel description for given reaction. The so obtained calculations enhance the magnitude of the fusion cross sections particularly in below barrier energy regimes but unable to recover the fusion excitation function data. The projectile is oblate in shape so the rotational states of projectile (2^+) as well as the one phonon 2^+ and 3^- vibrational states of target are incorporated in code CCFULL but the obtained results deviate from the sub-barrier fusion data. Besides that the excitation energy for the quadrupole vibrations is smaller than that of the octupole vibrations, the influence of octupole vibrations on the fusion process seems to be large therefore one phonon 2^+ and two phonon 3^- vibrational states along with quadrupole deformation (2^+) of projectile reproduced the sub-barrier fusion enhancement of the chosen reaction as shown in Fig. 1(a). Such outcomes slightly overestimate the fusion data at energies close to the barrier energy while at well above the Coulomb barrier, these calculations adequately explained the experimental data. For the ^{28}Si + ^{90}Zr reaction, all the nucleon (or multinucleon) transfer channels have negative ground state Q values so the possibilities of nucleon (multinucleon) transfer channels can be ruled out completely. Kalkal *et al.* [61,62], pointed out that there exists an α-pickup channel with a small positive ground Q value of $Q = +0.28$ MeV, but a magnitude of fusion enhancement at below barrier energies is quite insensitive to the coupling of such a channel. In this case, the nucleon transfer channels have a very small probability due to the neutron shell closure in the target and as a result of it, the effects of nucleon transfer channels are found to be suppressed. Therefore, the impacts of the collective inelastic surface vibrational states are more evident and hence by considering them, one can

TABLE II. The barrier characteristics like V_{B0}, R_B, and $\hbar\omega$ as used in the EDWSP model for calculations of fusion cross sections for various heavy ion fusion reactions.

System	V_{B0}(MeV)	R_B(fm)	$\hbar\omega$(MeV)	Reference
^{28}Si + ^{90}Zr	72.06	10.42	3.85	[64]
^{28}Si + ^{92}Zr	71.76	10.47	3.90	[64]
^{28}Si + ^{94}Zr	71.46	10.52	3.98	[64]
^{28}Si + ^{96}Zr	70.87	10.61	4.15	[64]

TABLE III. Range, depth, and diffuseness of standard Woods-Saxon potential used in the coupled channel calculations for various heavy ion systems [64].

System	r_0 (fm)	V_0(MeV)	a (fm)
^{28}Si + ^{90}Zr	1.170	68.00	0.66
^{28}Si + ^{92}Zr	1.170	68.25	0.66
^{28}Si + ^{94}Zr	1.170	68.50	0.66
^{28}Si + ^{96}Zr	1.180	67.82	0.66

TABLE IV. Range, depth, and diffuseness of the energy dependent Woods-Saxon potential for the calculations of various heavy ion fusion reactions [65–73].

System	r_0(fm)	V_0(MeV)	$\frac{a^{\text{Present}}}{\text{Energy Range}}(\frac{\text{fm}}{\text{MeV}})$
^{28}Si + ^{90}Zr	1.080	84.23	$\frac{0.96\text{ to }0.85}{64\text{ to }94}$
^{28}Si + ^{92}Zr	1.095	86.11	$\frac{0.96\text{ to }0.85}{64\text{ to }90}$
^{28}Si + ^{94}Zr	1.100	87.94	$\frac{0.97\text{ to }0.85}{62\text{ to }95}$
^{28}Si + ^{96}Zr	1.118	89.72	$\frac{0.98\text{ to }0.85}{61\text{ to }94}$

TABLE V. Q values (MeV) for ground state to ground state neutron pickup transfer channels for various heavy ion systems taken from Refs. [59–63].

System	$+1n$	$+2n$	$+3n$	$+4n$	$+5n$	$+6n$
$^{28}Si + ^{90}Zr$	−3.50	−2.20	−7.96	−8.37		
$^{28}Si + ^{92}Zr$	−0.16	+3.25	−2.13	−2.24		
$^{28}Si + ^{94}Zr$	+0.25	+4.13	+2.08	+4.09		
$^{28}Si + ^{96}Zr$	+0.62	+4.77	+3.13	+5.60	+1.47	+1.79

reasonably address the observed fusion enhancement of chosen reaction around the Coulomb barrier as depicted in Fig. 1(a).

In the case of the $^{28}Si + ^{92}Zr$ reaction, no-coupling predictions obtained by using the coupled channel code CCFULL are an order of magnitude smaller than experimental data and in order to remove discrepancies between fusion data and no-coupling outcomes, one has to consider internal structure degrees of freedom associated with the fusing systems. As the target is spherical in its ground state while the projectile has an oblate shape in its ground state, the vibrational excitations for the target and the quadrupole deformation for the projectile are the important for the fusion dynamics of a given reaction. The coupling to one phonon 2^+ and 3^- vibrational states of the target alone is not able to retrace the fusion cross-section data at below barrier energies. Since the excitation energy of quadrupole vibrations in the target is smaller than that of the octupole vibrations, its effects are expected to affect the theoretical outcomes. To improve the theoretical predictions, two phonon 2^+ and one phonon 3^- along with their mutual coupling such as $(2^+)^2$, $(2^+ \otimes 3^-)$ vibrational states in the target (^{92}Zr) are considered and these outcomes are also unable to recover the fusion excitation function data at sub-barrier energies. Further, three phonon 2^+ and one phonon 3^- vibrational states and their mutual couplings along with the 2^+ deformation of the projectile have been entertained in the coupled channel description but these calculations deviate from the fusion data particularly in below barrier energy regions as evident from Fig. 1(b). The discrepancies between the coupled channel predictions and the below barrier fusion data can be understood in terms of nucleon (multinucleon) transfer channels with positive ground state Q values. The two neutron pickup channel with positive ground state Q value equal to +3.25 MeV exists for the $^{28}Si + ^{92}Zr$ reaction, which must be incorporated for addressal of the fusion mechanism of the studied reaction. As the code CCFULL includes the neutron transfer channels approximately, in order to highlight the importance of the neutron transfer channels we have not considered such a transfer channel in the coupled channel analysis. In this case, an adequate explanation of the sub-barrier fusion anomalies cannot be achieved if one ignores the transfer channels and hence only entertains the collective excitations for fusing pairs. This directly points to the significance of the nucleon transfer channels for the fusion of the $^{28}Si + ^{92}Zr$ reaction.

TABLE VI. Q values (MeV) for ground state to ground state for transfer of proton, neutron, and alpha particle for various heavy ion systems taken from Refs. [59–63].

System	$+1p$	$-1p$	$-1n$	$-\alpha$	$+\alpha$
$^{28}Si + ^{90}Zr$	−5.60	−6.43	−9.98	−7.92	+0.28
$^{28}Si + ^{92}Zr$	−6.65	−5.54	−10.44	−7.22	+3.99
$^{28}Si + ^{94}Zr$	−7.58	−4.78	− 10.72	−6.71	+3.20

In the case of the $^{28}Si + ^{94}Zr$ reaction, the same coupling scheme as tested for the $^{28}Si + ^{90}Zr$ system has been utilized to reproduce the fusion of $^{28}Si + ^{94}Zr$ reaction, but such a coupling scheme fails to address the fusion enhancement at near and sub-barrier energies. The no-coupling case strongly underpredicts the experimental data at below barrier energies. The considerations of one phonon 2^+ and 3^- vibrational states along with their mutual couplings bring a large fusion cross section with respect to the no-coupling scheme. But the sub-barrier fusion data could not be addressed with such calculations. The significantly large discrepancies between the calculated results and fusion cross-section data at below barrier energies thereby suggest taking the impacts of more intrinsic channels in order to explain the experimental data. Since the excitation energy of the quadrupole vibrations of the target is sufficiently lower than that of its octupole vibrations, the inclusion of two phonon 2^+ and one phonon 3^- vibrational states enhances the magnitude of the fusion cross sections relative to the no coupling case but fails to recover the data at sub-barrier energies. In our calculations, we have also tested the effects of one phonon 2^+ and two phonon 3^- vibrational states in the target and the quadrupole deformation in projectile (2^+) along with their mutual couplings, which enhances the fusion cross sections, however still there are large deviations between theoretical outcomes and the experimental data [see Fig. 2(a)]. This demand for further addition of more intrinsic channels is associated with the participant nuclei. The considerations of three phonon 3^- and one phonon 2^+ along with their mutual coupling such as $(3^-)^2$, $(3^-)^3$, $(2^+ \otimes 3^-)$, and $[2^+ \otimes (3^-)^2]$ vibrational states and quadrupole deformation in projectile (2^+) improve the theoretical predictions but could not retrace fusion cross-section data particularly in sub-barrier energy regions. Such large deviations can be understood in terms of nucleon (or multinucleon) transfer channels.

For a given reaction, there exist a large number neutron transfer channels with positive ground state Q values (see Table V). $^{28}Si + ^{94}Zr$ reaction facilitates one neutron ($1n$), two neutron ($2n$), three neutron ($3n$), and four neutron ($4n$) transfer channels with positive ground state Q values. The Q values for $1n$, $2n$, $3n$, and $4n$ pickup channels are +0.25, +4.13, +2.08, and +4.09 MeV, respectively. In addition, an α-pickup channel with positive ground Q value of $Q = +3.99$ MeV also exists but the probability of transferring four neutrons is quite large in comparison to that of the other transfer channels. Hence, the deviations between the present coupled channel outcomes and experimental data in sub-barrier energy regimes can only be linked with such neutron transfer channels. Kalkal *et al.* [60–62] have explicitly shown that in addition to collective surface excitations associated with the

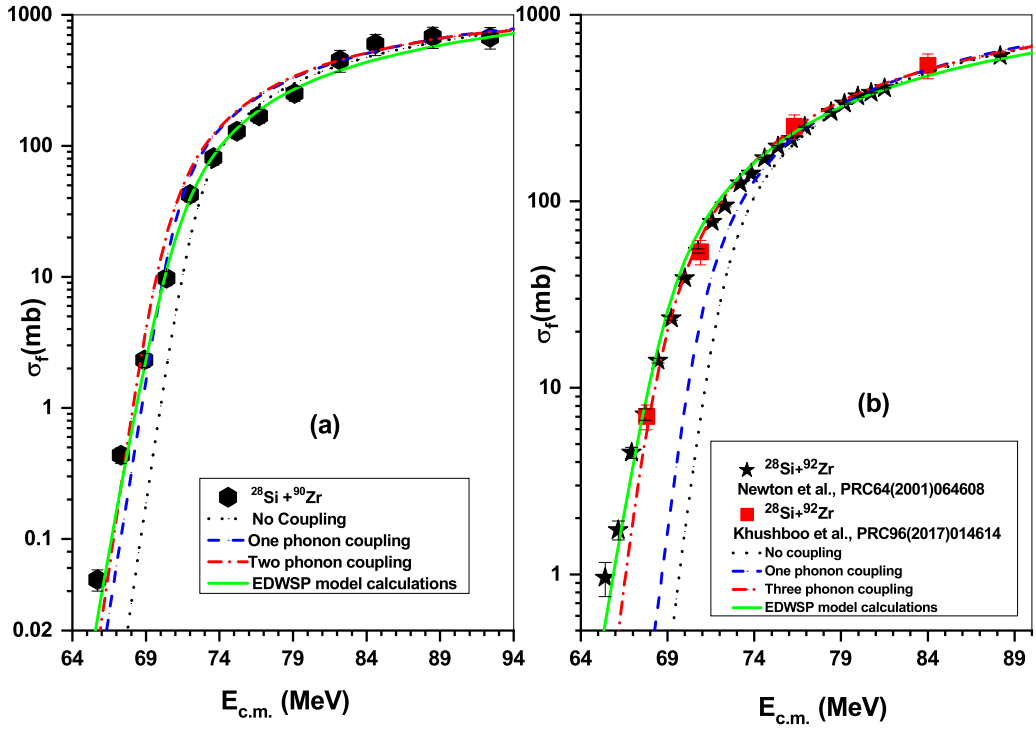

FIG. 1. The fusion excitation functions of ^{28}Si + ^{90,92}Zr reactions, which are obtained by using the EDWSP model [65–73] and the coupled channel code CCFULL [64]. The results are compared with the available experimental data taken from Refs. [59–63].

colliding partners, the couplings to neutron transfer channels with positive ground state Q values are necessarily required in order to account for the sub-barrier fusion enhancement. References [60–62] pointed out that one and two proton stripping may also affect the fusion cross-section data at energies well above the barrier. In this sense, the nucleon (or multinucleon)

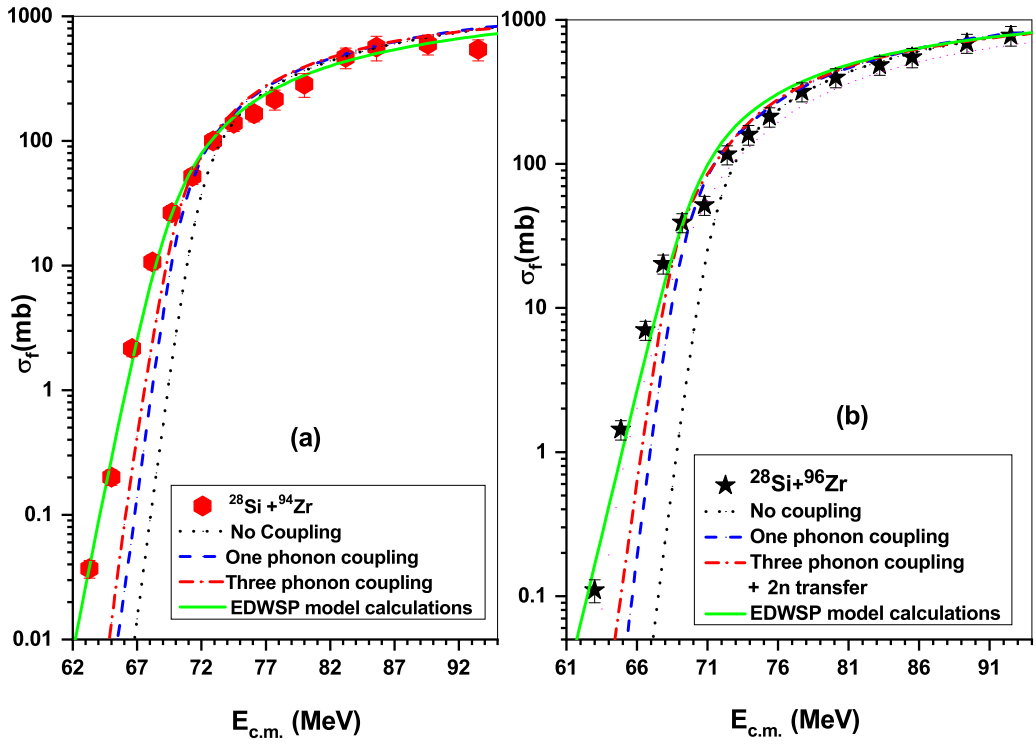

FIG. 2. Same as Fig. 1 but for ^{28}Si + ^{94,96}Zr reactions. The results are compared with the available experimental data taken from Refs. [60,63].

transfer channels are turned out to be an important mode of couplings and hence dominate over the collective excitations in the fusion mechanism of the $^{28}Si + ^{94}Zr$ reaction as inferred from Fig. 2(a).

In the fusion of the $^{28}Si + ^{96}Zr$ reaction, the coupled channel calculations corresponding to the no coupling case remain significantly smaller than that of the experimental data. The couplings to low lying states like one phonon 2^+ and 3^- vibrational states along with their mutual couplings improve the theoretical results as such calculations increase the fusion cross sections by several orders of magnitude over the no coupling case. The strength of octupole vibrations is quite large and its excitation energy is significantly lower than the corresponding value in other targets. Therefore, the octupole vibrations in a heavier target (^{96}Zr) are strongest and its influences on the fusion process of the present reaction cannot be ignored and hence is expected to be quite large. The considerations of three phonon 3^- vibrational state alone bring a large enhancement over that of the 2^+ vibrational state but so obtained calculations could not address the sub-barrier fusion data and hence are not shown in Fig. 2(b). The inclusions of four phonon 3^- vibrational states seem to be insensitive and unable to bring the required magnitude of the experimental data. The large deviations between such calculations and sub-barrier fusion data demand more intrinsic channels for explanation of the fusion enhancement at below barrier energies. The theoretical outcomes obtained by taking one phonon 2^+ and three phonon 3^- vibrational states of the target along their mutual couplings like $(3^-)^2$, $(2^+ \otimes 3^-)$, $[(2^+) \otimes (3^-)^2]$, and quadrupole deformation in projectile fail to describe the fusion data at below barrier energies and hence these outcomes are also not shown. The present reaction offers many neutron (or multineutron) transfer channels with positive ground state Q values. The Q values for $1n$, $2n$, $3n$, $4n$, $5n$, and $6n$ pickup channels are $+0.62$, $+4.77$, $+3.13$, $+5.60$, $+1.4$, and $+1.79$ MeV, respectively. The code CCFULL considers the transfer channels in an approximate way and there is a provision of addition of a two neutron pickup channel so the present coupled channel calculations are performed by including one phonon 2^+ and three phonon 3^- vibrational states in the target, quadrupole deformation in projectile (2^+), and a two neutron pickup channel with a coupling strength of $F_t = 0.5$ MeV but so obtained calculations are unable to address the observed fusion enhancement at below barrier energies as evident from Fig. 2(b). The coupling strength (F_t) for transfer channel can be adjusted to gain better agreement with data. The coupling strength $F_t = 0.5$ MeV provides the best fit to experimental data at above barrier energies. As the code CCFULL does not consider the coupling to all transfer channels simultaneously, the effects of the all neutron transfer channels cannot be analyzed properly by using the present coupled channel calculations. In order to achieve a good description to fusion data, it is necessary to include the all the neutron transfer channels along with the collective excitations in the target as well as in the projectile. The additional neutron tries to deform the shape of the nucleus during collision and subsequently decreases the height of the Coulomb barrier resulting in the larger penetration probability. In other words, the neutron transfer forms neck between the projectile and target and the fusion process is initiated in the neck region by a neutron flow between the projectile and target before fusion. Such neutron transfer with positive Q value results in an increase of kinetic energy of relative motion and consequently fusion is favored [50]. More are neutron rich participants; the larger is the separation distance at which collision partners may fuse and the thinner is the dynamical fusion barrier. Therefore, the influences of multinucleon transfer channels on the fusion process are expected to be significant and such effects are found to increase as one moves from a lighter target (^{90}Zr) to a heavier target (^{96}Zr). In this sense, the impacts of nucleon (or multinucleon) transfer channels dominate over the collective excitations associated with the collision partners, henceforth responsible for an anomalously large fusion enhancement for $^{28}Si + ^{96}Zr$ reaction particularly at below barrier energies as inferred from Fig. 2(b). Henning *et al.* [90], suggested that the fusion enhancement due to neutron transfer channels becomes unambiguously clear if one deals with the Q_{opt} value (optimum Q value) instead of dealing with the positive ground state Q value. This is because in some cases the ground sate Q value is positive while the corresponding Q_{opt} value is negative and thus the fusion dynamics remains almost insensitive to such multinucleon transfer channels. That is why, in some cases, besides the existence of neutron transfer channels with positive ground state Q values, the strong isotopic fusion enhancements are not reflected even if one bombards a common projectile on a series of target isotopes and vice versa.

B. EDWSP model analysis

The total interaction potential between colliding nuclei is made up of three terms; Coulomb potential, nuclear potential, and centrifugal potential. The nominal Coulomb barrier ($\ell = 0$ for which the centrifugal term becomes zero) between the collision partners has to be penetrated by the interacting nuclei for the occurrence of the complete fusion events. Generally, the conventional Woods-Saxon type, which is independent of the energy, has been adopted for analyzing the nuclear interactions between collision partners. As pointed out in the literature [7,76,77], there are considerably large uncertainties in the parameters of Woods-Saxon potential for description of the different types of nuclear interactions. Further, it has been emphasized that the static Woods-Saxon potential fails in simultaneous explanation of elastic scattering data and heavy ion fusion reactions data and the cause of this is still unknown [7,76,77]. The outcomes of the one dimensional BPM obtained by taking the static Woods-Saxon potential deviate appreciably from the experimental findings particularly at sub-barrier energies. In such a case, the behaviors of the fusion excitation can only be judged if one considers the nuclear structure degrees of freedom associated with the collision pairs and the same is true for chosen reactions as evident from Figs. 1 and 2. In the eigenchannel model [8–13,56–58,76–85,91,92], the coupling between the elastic channel and internal structure degrees of freedom of the projectile and target results in the splitting of the nominal barrier into a distribution of barriers of different weights and heights. These barriers are distributed

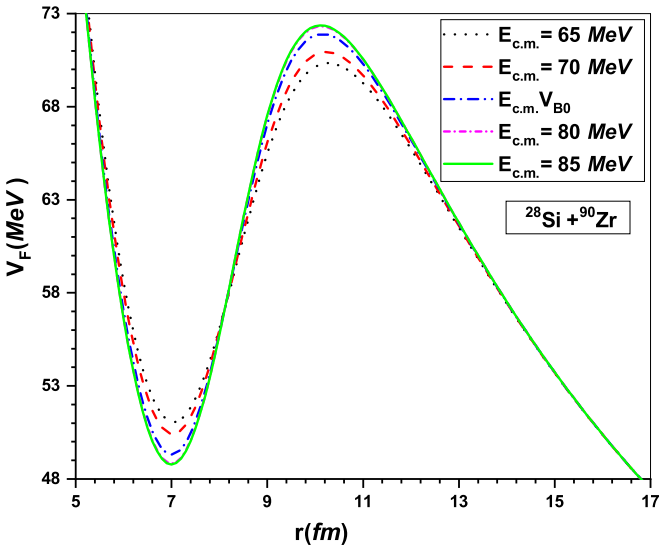

FIG. 3. The fusion barrier (FB) for ^{28}Si + ^{90}Zr system obtained by using the EDWSP model [65–73].

about an average barrier and the weight of the barrier represents its corresponding probability encountering that barrier. In general, the maximum numbers of the intrinsic channel that can be included in the coupled channel approach are limited to some extent. Alternatively, many other theoretical approaches [1–3,8–13,56–58,76–85,91,92] have been utilized to explore the fusion dynamics of stable and weakly bound nuclei.

In the EDWSP model, the energy dependent diffuseness generates effective energy dependent fusion barriers at different bombarding energies. This leads to a spectrum of fusion barriers of variable weights and heights as shown in Figs. 3 and 4. In this spectrum, the heights of some of the energy dependent fusion barriers are lower than that of the Coulomb barrier and thereby allow the passage of the flux from the

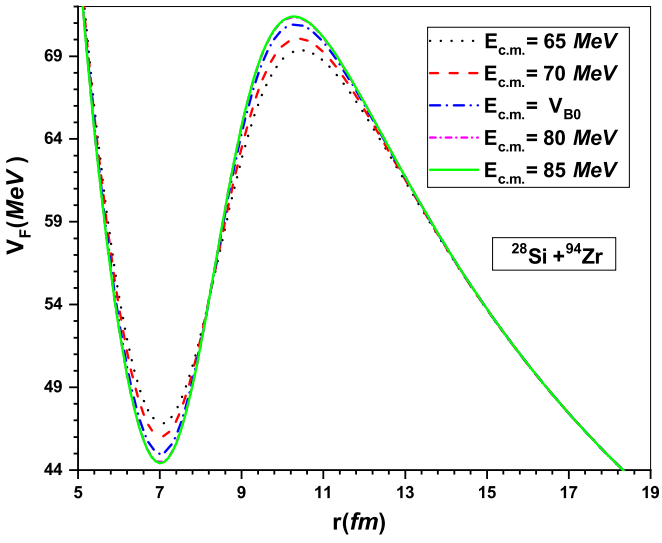

FIG. 4. Same as in Fig. 3 but for ^{28}Si + ^{94}Zr system. The similar results are found for ^{28}Si + ^{92,96}Zr reactions.

elastic channel to the fusion channel. Subsequently, the EDWSP model calculations predict larger fusion cross sections at sub-barrier energies in comparison to the outcomes of one dimensional BPM. In this way, the EDWSP based outcomes are nearer to the fusion data and appropriately explain the observed fusion enhancement of a given reaction under study. The other underlying reason that the present model adequately describes the behaviors of fusion cross-section data for chosen reactions is that the diffuseness parameter is also related to the barrier width and the channel coupling strengths. The channel coupling strengths for collective excitations, static deformation, and higher order deformations and/or nucleon transfer channels are directly linked with the first order derivate of nuclear potential ($F_N(r)$ or $F_{\text{Transfer}}(r) \propto \frac{dV_N(r)}{dr}$) [8–13,56–58,76–85,91,92]. In this sense, the variation in diffuseness parameter directly or indirectly affects barrier width as well as channel coupling strengths and subsequently modifies the barrier characteristics in such a way that there is a barrier lowering phenomenon. The modification of barrier characteristics is the key ingredient of the EDWSP model and consequently the dominant channel coupling effects produced due to nuclear structure effects are now well accommodated by the energy dependent interaction potential. The barrier modifications for ^{28}Si + ^{90,94}Zr reactions are shown in Figs. 3 and 4. Similar results are found for ^{28}Si + ^{92,96}Zr reactions and hence are not shown here.

The difference in the structural properties of targets can also be noticed from the EDWSP based calculations. For the ^{28}Si + ^{90}Zr reaction, all the neutron transfer channels have negative ground state Q values and thus their influences on fusion process are suppressed. However, in the case of the ^{28}Si + ^{94}Zr reaction, due to more and more open transfer channels with a positive ground state Q value, the transferring of a neutron (multineutron) is expected to start at larger internuclear separations between collision partners. As a result, a longer tail of the interaction barrier is expected for the ^{28}Si + ^{94}Zr reaction relative to the ^{28}Si + ^{90}Zr reaction and hence the same is inferred from Figs. 3 and 4. This clearly intimates the dominance of neutron (multineutron) transfer channels in the neutron rich target. A similar trend of fusion barrier is also found for ^{28}Si + ^{92,96}Zr reactions. Such physical effects can also be understood in terms of the range parameters (see Table IV) used in the EDWSP model for estimations of the fusion cross sections. The increasing values of the range parameter from $r_0 = 1.080$ to 1.118 fm as one moves from a ^{28}Si + ^{90}Zr to ^{28}Si + ^{96}Zr reaction is indicative of the importance of the neutron transfer couplings in the latter system. Further, the importance of vibrational couplings and/or neutron transfer couplings can also be understood in terms of the effective fusion barrier between reacting nuclei. From Figs. 3 and 4, one can easily notice that at lowest incident energy, the lowest energy dependent fusion barrier is produced. This is due to the fact that at the lowest incident energy, the diffuseness is largest [$a =$ 0.96 fm for ^{28}Si + ^{90,92}Zr and $a = 0.97$ fm ($a = 0.98$ fm) for ^{28}Si + ^{94}Zr (^{28}Si + ^{96}Zr)] which in turn generates the barrier lowering effects. The smallest energy dependent fusion barrier (FB) for ^{28}Si + ^{90}Zr (^{28}Si + ^{92}Zr) is FB = 70.04 MeV (FB = 68.30 MeV) while for ^{28}Si + ^{94}Zr (^{28}Si + ^{96}Zr) it is

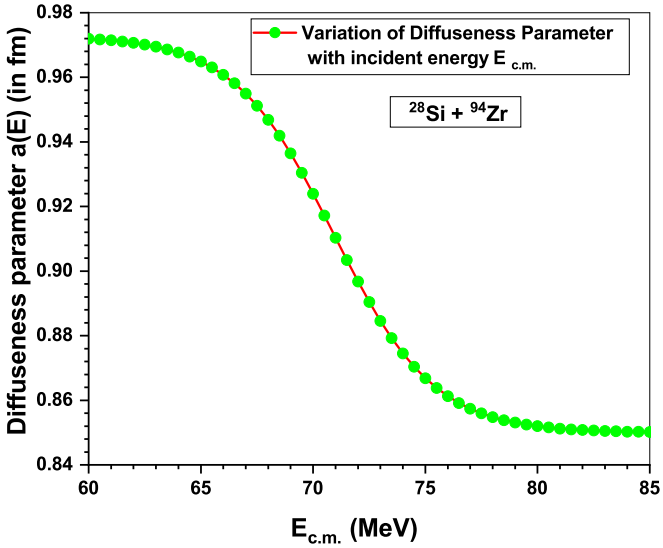

FIG. 5. Variation of energy dependent diffuseness parameter with center of mass energy for ^{28}Si + ^{94}Zr reaction, which is obtained by using the EDWSP model.

FB = 68.08 MeV (FB = 69.16 MeV). The so produced fusion barriers are much smaller than that of the Coulomb barrier for given reactions (see Table II) and further supplement the shifting of elastic flux into the fusion channel. In this way model predictions lead to the larger fusion cross sections in near and below barrier energy regimes. In the literature, experimental measurements for many fusing systems have shown that the fusion cross-section data get saturated in above barrier energy regions [1–3,8–13,56–58,76–85,91,92]. This physical effect has been adequately incorporated in the EDWSP model, wherein the variation of diffuseness gets saturated to its lowest value in above barrier energy regimes ($a = 0.85$ fm). This saturation in diffuseness automatically ceases the change in the height of the energy dependent fusion barrier at above barrier energies, which in turn intimates insensitivity of the above barrier fusion data towards the channel coupling effects associated with the fusing partners. The variation of energy dependent diffuseness parameter with center of mass energy that governs barrier modulation effects in the EDWSP model is shown in Fig. 5 for ^{28}Si + ^{94}Zr reaction. A similar trend of variation in diffuseness parameter is found for other fusing systems.

Umar and co-workers [84,85], using the density-constrained time-dependent Hartree-Fock theory (DC-TDHF), showed that the channel coupling effects and the coordinate-dependent mass modify the nucleus-nucleus potential and induce energy dependence in the nucleus-nucleus potential. As a result of dynamical lowering of the fusion barrier, the DC-TDHF approach adequately explained the fusion dynamics of various heavy ion fusion reactions. Wang *et al.* [93,94], using the improved quantum molecular dynamical (ImQMD) model analyzed the fusion dynamics of neutron rich nuclei such as ^{40,48}Ca + ^{90,96}Zr reactions and concluded that neutron transfer between the interacting nuclei takes place at a larger distance (just before fusion). The formation of a neck [95] between projectile and target reduces the dynamical fusion barrier in comparison to the normal static fusion barrier between fusing pairs. Similar conclusions were also drawn by the authors based upon the mean field transport theory [96], wherein authors obtained good fits to the fusion dynamics of ^{16}O + ^{16}O and ^{58}Ni + ^{58}Ni reactions. In the EDWSP model, the closely similar aforementioned physical effects have been noticed for the studied reactions. In close resemblance to the coupled channel approach, the ImQMD model and the DC-TDHF, the barrier modifications produced in the EDWSP model result in the predictions of larger sub-barrier fusion cross sections and hence adequately describe the fusion dynamics of given reactions. Although the EDWSP model explicitly does not consider the effects of the collective excitations, permanent shape deformation and higher order deformation of the projectile (or target or both), and/or nucleon transfer channels or other channel coupling effects, due to the dynamical nature of the energy dependent interaction potential, all such physical effects are intrinsically included in the EDWSP calculations.

TABLE VII. χ^2 values for the fusion dynamics of ^{28}Si + ^{90,92,94,96}Zr reactions obtained for the EDWSP model calculations.

System	χ^2-value (EDWSP model)	Dominance of type of coupling (vibrational/transfercoupling)
^{28}Si + ^{90}Zr	3.02	vibrational coupling
^{28}Si + ^{92}Zr	2.82	vibrational and transfer coupling
^{28}Si + ^{94}Zr	2.98	transfer coupling
^{28}Si + ^{96}Zr	3.14	transfer coupling

C. χ^2 analysis of the fusion cross sections

For theoretical outcomes, the goodness of fit can be judged by χ^2 analysis, which can be obtained by using the following relation [32,71,72]:

$$\chi^2 = \frac{1}{N}\sum_{i=1}^{N}\left[\frac{\{\sigma_{\rm Expt}(E_i) - \sigma_{\rm Model}(E_i)\}^2}{\sigma_{\rm Model}(E_i)}\right],$$

where N are the number of data points, E_i are the experimental energies at which measurements have been carried out, $\sigma_{\rm Expt}$ and $\sigma_{\rm Model}$ are the experimental and model cross sections respectively. χ^2 measures the deviation of theoretical predictions from the fusion data. The present χ^2 analysis includes the experimental uncertainties of the data and has been done for EDWSP calculations. The extracted χ^2 values for ^{28}Si + ^{90,92,94,96}Zr reactions are listed in Table VII. The χ^2 values for ^{28}Si + ^{90}Zr, ^{28}Si + ^{92}Zr, ^{28}Si + ^{94}Zr, and ^{28}Si + ^{96}Zr reaction are 3.02, 2.82, 2.98, and 3.14, respectively, which are consistent with the fact that experimental data are well reproduced by the model calculations. In other words, the smaller χ^2 values obtained for studied reactions highlighted that the EDWSP predictions provide a fine tuning to experimental data.

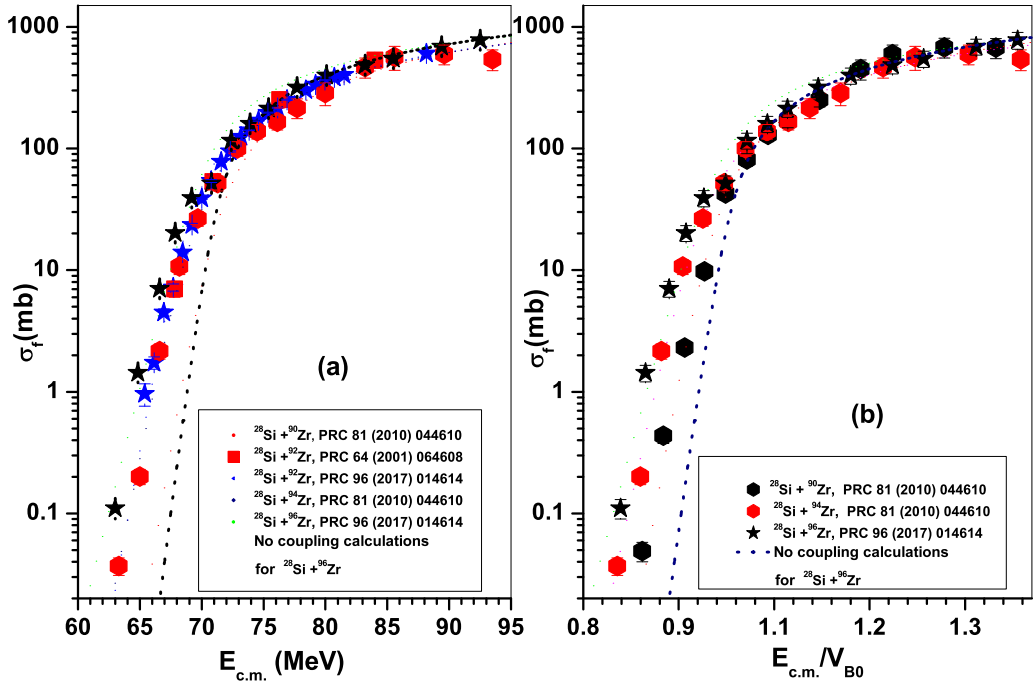

FIG. 6. The fusion cross-section data of $^{28}\mathrm{Si} + {}^{90,92,94,96}\mathrm{Zr}$ reactions (a) and $^{28}\mathrm{Si} + {}^{90,94,96}\mathrm{Zr}$ reactions (b) are compared with each other and also compared with no-coupling calculations obtained by using the code CCFULL [64]. The experimental data are taken from Refs. [59,60,63].

D. Comparison of experimental data with similar systems

In order to disentangle the role of the neutron transfer couplings from the vibrational couplings associated with the collision pairs in the fusion process, the experimental data of present reactions are compared with those of similar systems. In the case of both reaction partners having almost similar collective strengths, then the impacts of transfer channels are directly reflected from the comparison of the experimental data. In this regard, the fusion excitation functions data for $^{28}\mathrm{Si} + {}^{90,92,94,96}\mathrm{Zr}$ reactions are compared in Fig. 6(a) and for $^{28}\mathrm{Si} + {}^{90,94,96}\mathrm{Zr}$ reactions are compared in Fig. 6(b). As already discussed, the different behaviors of the fusion excitation functions for $^{28}\mathrm{Si} + {}^{90,92,94,96}\mathrm{Zr}$ reactions can be attributed to the contribution of collective excitations of targets and/or neutron (multineutron) transfer channels with positive ground state Q values to the fusion process. Based on collective properties, one can realize that the heavier target (^{96}Zr) exhibits strong octupole vibrations and its influences seem to be strongest in the fusion of $^{28}\mathrm{Si} + {}^{96}\mathrm{Zr}$ reaction. Further, with the increase of neutron richness, more and more neutron (multineutron) transfer channels with positive ground state Q values are opened up. This makes the neutron transfer more probable, henceforth their impacts are also strongest in a heavier target (^{96}Zr). Due to the presence of a $2n$-pickup channel with a positive Q value for the $^{28}\mathrm{Si} + {}^{92}\mathrm{Zr}$ reaction, there is a larger sub-barrier fusion enhancement for $^{28}\mathrm{Si} + {}^{92}\mathrm{Zr}$ relative to $^{28}\mathrm{Si} + {}^{90}\mathrm{Zr}$ reaction. For the $^{28}\mathrm{Si} + {}^{94}\mathrm{Zr}$ reaction, the probabilities of up to four neutron pickup channels are large, which in turn is responsible for an appreciably large fusion enhancement for this reaction over the $^{28}\mathrm{Si} + {}^{92}\mathrm{Zr}$ reaction. In the case of the $^{28}\mathrm{Si} + {}^{96}\mathrm{Zr}$ reaction, the existence of $1n$ to $6n$ pickup channels thereby significantly increases the magnitude of the fusion enhancements at below barrier energies in comparison to that of the $^{28}\mathrm{Si} + {}^{94}\mathrm{Zr}$ reaction (Fig. 6).

For more concrete conclusions, the fusion data for $^{28}\mathrm{Si} + {}^{90,92,94,96}\mathrm{Zr}$ reactions are also compared along with EDWSP calculations and are shown in Fig. 7. From the comparison (EDWSP based fusion cross-section as well as fusion cross-section data), one suggests that the fusion

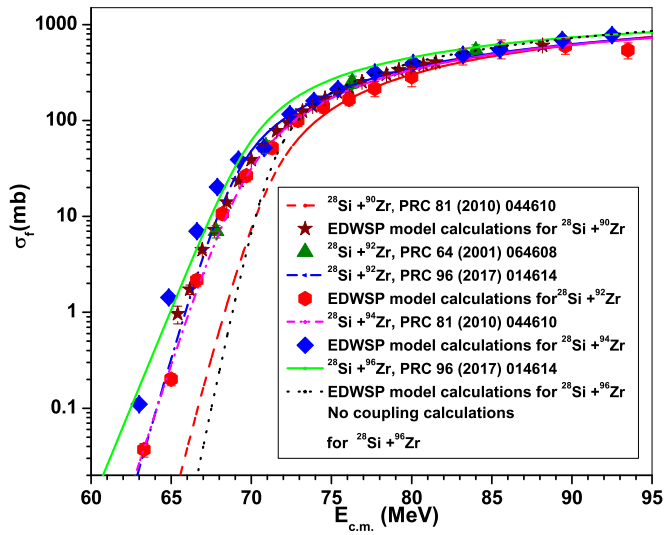

FIG. 7. The fusion excitation functions of $^{28}\mathrm{Si} + {}^{90,92,94,96}\mathrm{Zr}$ reactions are compared along with theoretical predictions obtained by using the EDWSP model [65–73]. The results are compared with available experimental data taken from Refs. [59–60,63].

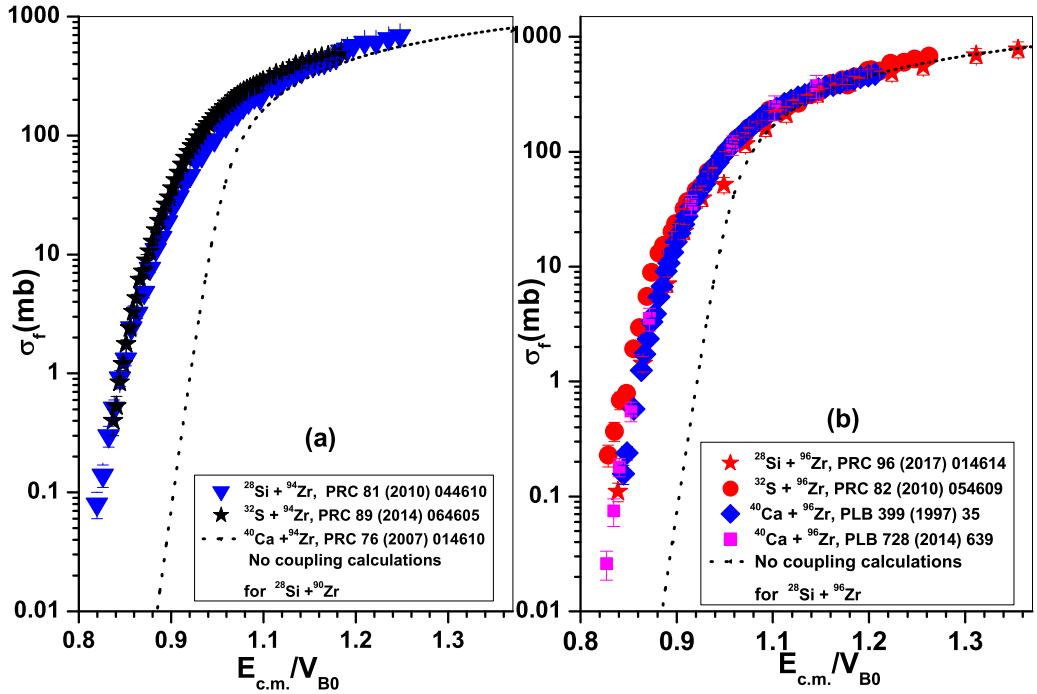

FIG. 8. The fusion cross-section data for ^{28}Si + ^{94}Zr, ^{32}S + ^{94}Zr, and ^{40}Ca + ^{94}Zr reactions (a) and for ^{28}Si + ^{96}Zr, ^{32}S + ^{96}Zr, and ^{40}Ca + ^{96}Zr reactions (b) are compared along with the no-coupling calculations obtained by using the code CCFULL [64]. The results are compared with available experimental data taken from Refs. [39–42,59–63,97].

enhancements at sub-barrier energies for the ^{28}Si + ^{96}Zr reaction are significantly larger than that of ^{28}Si + ^{90,92,94}Zr reactions. In the case of the ^{28}Si + ^{94}Zr reaction, the magnitude of fusion enhancements at below barrier energies is much greater than that of ^{28}Si + ^{90,92}Zr reactions. The sub-barrier fusion enhancement of the ^{28}Si + ^{92}Zr reaction is larger than that of the ^{28}Si + ^{90}Zr reaction. The similar behaviors of fusion cross sections as inferred from Fig. 6 can be noticed from that of Fig. 7. Such a trend of the fusion cross sections is the consequence of the combined effects of vibrational couplings and neutron transfer couplings. This directly clarified the strong target isotopic dependence of sub-barrier fusion enhancements of ^{28}Si + ^{90,92,94,96}Zr reactions.

To single out the importance of the vibrational couplings and/or transfer couplings, the comparison of the fusion data for the ^{28}Si + ^{94}Zr reaction has been done with that of similar systems like ^{32}S + ^{94}Zr and ^{40}Ca + ^{94}Zr reactions [see Fig. 8(a)]. In a similar sense, the fusion cross-section data of the ^{28}Si + ^{96}Zr reaction are shown along with that of ^{32}S + ^{96}Zr and ^{40}Ca + ^{96}Zr reactions [see Fig. 8(b)]. From Fig. 8(a), one can say that fusion data for ^{32}S + ^{94}Zr and ^{40}Ca + ^{94}Zr reactions are appreciably larger than that of the ^{28}Si + ^{94}Zr reaction, which in turn is significantly larger than the no-coupling case. Although there exist four neutron (multineutron) transfer channels with positive ground state Q values for all three systems, the influences of the transfer channels and collective degrees of freedom are more pronounced in the case of ^{32}S + ^{94}Zr and ^{40}Ca + ^{94}Zr reactions. Due to different collective and nuclear structure properties of the projectiles, the combined effects of the vibrational couplings and neutron transfer couplings become dominant one and hence the fusion cross sections are enhanced for ^{32}S + ^{94}Zr and ^{40}Ca + ^{94}Zr reactions relative to the ^{28}Si + ^{94}Zr reaction [see Fig. 8(a)]. Similar trends of fusion cross sections turned out for ^{32}S + ^{96}Zr, ^{40}Ca + ^{96}Zr, and ^{28}Si + ^{96}Zr reactions, wherein the fusion data of ^{32}S + ^{96}Zr and ^{40}Ca + ^{96}Zr reactions are found to be much larger than that of the ^{28}Si + ^{96}Zr reaction [see Fig. 8(b)]. Hence, the sub-barrier fusion enhancement due to multineutron transfer channels with positive ground state Q values is more evident for ^{32}S + ^{96}Zr and ^{40}Ca + ^{96}Zr relative to ^{28}Si + ^{96}Zr systems.

It is believed that the various kinds of channel coupling effects are only active at sub-barrier energies while such physical effects are unimportant in above barrier energy regions. Therefore, the above barrier fusion data should be accurately analyzed within the framework of one dimensional BPM [1–3,8–13,56–58,76–85,91,92]. Newton *et al.* [76], obtained the good fits to the above barrier fusion data for varieties of projectile-target systems and concluded that abnormally larger values of diffuseness parameter ($a = 0.75$–1.5 fm) of standard Woods-Saxon potential are required to reproduce the above barrier experimental data. Chushnyakova *et al.* [98–100], using the trajectory fluctuation dissipation (TFD) model, which is based upon the parametrization of *SKP* and *SKX* Skyrme forces, appropriately described the fusion dynamics of a wide range of projectile-target combinations and hence achieved an agreement with the experimental cross-section data within 10% with a probability greater than 90%. Following this point, the predictions based on EDWSP model

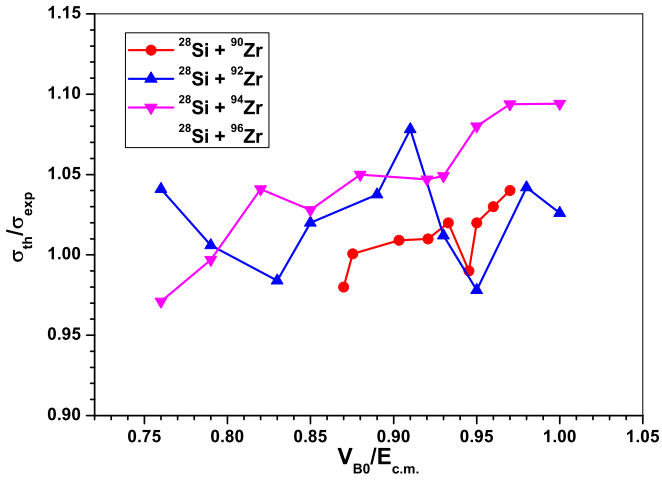

FIG. 9. The ratio of $\xi = \frac{\sigma_{\text{theor}}}{\sigma_{\text{expt}}}$ as the function of $\frac{V_{B0}}{E_{\text{c.m.}}}$ for studied reactions.

calculations in above barrier energy regions are shown in Fig. 9. The experimental data of $^{28}\text{Si} + ^{90,92,94,96}\text{Zr}$ reactions have the precision of about 10% at energies above the Coulomb barrier and the parameters of static Woods-Saxon potential as used in Refs. [59,60,63] were chosen from the fitting of the above barrier fusion data. For these fusing systems, the EDWSP model is able to reproduce the above barrier portion of the fusion data within 5% with probability larger than 90%. For studied systems, 33 fusion data points out of 38 fusion data points lie within 5% while 5 fusion data points lie within 10%. In the above barrier energy regions, the EDWSP model has reached a close agreement with fusion data and hence suggest that the EDWSP model adequately addresses the experimental data for given reactions. In other words, at above barrier energies the TFD model and the EDWSP model have a close resemblance in their predictive power.

IV. CONCLUSIONS

This work analyzed role of collective excitations associated with collision partners and/or neutrons transfer channels in the fusion dynamics of $^{28}\text{Si} + ^{90,92,94,96}\text{Zr}$ reactions by using the coupled channel approach and the EDWSP model. Within the coupled channel approach, it has been clarified that for $^{28}\text{Si} + ^{90}\text{Zr}$ reaction, the couplings to collective excitations are found to be more important and enhance fusion cross sections at below barrier energies by several orders of magnitude with respect to the no-coupling case, while for the $^{28}\text{Si} + ^{92}\text{Zr}$ reaction, the influences of collective surface vibrational modes of colliding systems as well as the neutron transfer channels with positive ground state Q value are necessarily required for the complete description of the fusion dynamics around the Coulomb barrier. The magnitude fusion enhancement at sub-barrier energies is larger for $^{28}\text{Si} + ^{92}\text{Zr}$ reaction relative to the $^{28}\text{Si} + ^{90}\text{Zr}$ reaction, which can be attributed to the possibilities of neutron transfer channels. In the case of $^{28}\text{Si} + ^{94}\text{Zr}$ reaction, there are $1n - 4n$ transfer channels and the fusion cross sections turn out to be quite sensitive to such neutron transfer channels. The experimental data cannot be reproduced just by considering the collective excitations and hence the couplings to neutron (or multineutron) transfer channels are needed in order to retrace the fusion data particularly in below barrier energy regimes. The larger sub-barrier fusion enhancement for $^{28}\text{Si} + ^{94}\text{Zr}$ reaction with reference to $^{28}\text{Si} + ^{90,92}\text{Zr}$ reactions can only be correlated with the large probability of neutron (multineutron) transfer channels with positive ground state Q values in the former system. For the $^{28}\text{Si} + ^{96}\text{Zr}$ reaction, the degree of fusion enhancement increases further with reference to that of $^{28}\text{Si} + ^{94}\text{Zr}$ reaction and consequently the order of sub-barrier fusion enhancement becomes much larger than that of $^{28}\text{Si} + ^{90,92,94}\text{Zr}$ reactions. Such characteristics of the former system can only be linked with the neutron transfer channels. In the case of the $^{28}\text{Si} + ^{96}\text{Zr}$ reaction, $1n-6n$ transfers are allowed with positive ground state Q values and the coupling to these transfer channels enhances the fusion cross sections at near and sub-barrier energies by several orders of magnitude with respect to the outcomes of one dimensional BPM.

The EDWSP based calculations also arrived at the aforementioned conclusions. In EDWSP model calculations, the increasing values of the range parameter clearly reflected that more and more barrier modifications are needed as one moves from a lighter target (^{90}Zr) to a heavier one (^{96}Zr). In this model, the range parameter is directly linked with the energy dependent diffuseness that produces the barrier lowering phenomenon. Calculations indicated that larger the value of the diffuseness parameter, greater are the barrier lowering effects that are induced which subsequently results in the predictions of larger fusion cross sections at near and below barrier energies. The increasing values of range parameter with the increase of target isotopic mass is also consistent from the nuclear structure point of view. As the isotopic mass of target increases, the target isotope becomes more and more soft due to the increase of coupling strength of octupole vibrations and the decrease of its excitation energy. In addition, the probabilities of neutron (multineutron) transfer channels with the positive ground state Q values become appreciably large with the increase of neutron richness. In the EDWSP model, the barrier lowering effects are main ingredients and subsequently, the present model calculations reasonably address the fusion data of $^{28}\text{Si} + ^{90,92,94,96}\text{Zr}$ reactions at energies spanning around the Coulomb barrier. This fact unambiguously clarified the dominance of transfer couplings over the collective excitations associated with the projectile and target systems. Although the EDWSP model explicitly does not consider the couplings to nuclear structure degrees of freedom like vibrational excitations and/or transfer channels but due to energy dependence in nature, it reasonably describes the sub-barrier fusion anomalies of chosen reactions. This intimates that the energy dependent interaction potential is an artifact masking of various dominant channel coupling effects in fusion dynamics of the studied reactions. Furthermore, the EDWSP based results are capable of achieving the above barrier portion of the fusion cross-section data within 5% with probability larger than 90%. For chosen reactions, the 33 fusion data points out of 38 fusion data points lie within 5% while the 5 fusion data points lie within the 10%. This clearly indicates that model calculations are able to give an

adequate description to the fusing data of studied reactions with a probability greater than 90%. In addition, smaller χ^2 values for EDWSP outcomes, which range from 2.82 to 3.14, suggested that the model calculations provide good tuning with the fusion data and hence point towards the adequacies of the adopted model.

[1] S. G. Steadman and M. J. Rhoades Brown, Annu. Rev. Nucl. Part. Sci. **36**, 649 (1986).
[2] M. Beckerman, Rep. Prog. Phys. **51**, 1047 (1988).
[3] J. R. Leigh *et al.*, Phys. Rev. C **52**, 3151 (1995).
[4] M. S. Gautam, Phys. Scr. **90**, 125301 (2015).
[5] A. M. Vinodkumar *et al.*, Phys. Rev. C **53**, 803 (1996).
[6] N. V. S. V. Prasad *et al.*, Nucl. Phys. A **603**, 176 (1996).
[7] M. S. Gautam, Phys. Scr. **90**, 055301 (2015).
[8] M. Dasgupta, D. J. Hinde, N. Rowley, and A. M. Stefanini, Annu. Rev. Nucl. Part. Sci. **48**, 401 (1998).
[9] M. S. Gautam, Phys. Scr. **90**, 025301 (2015).
[10] W. Reisdorf, J. Phys. G **20**, 1297 (1994).
[11] L. F. Canto *et al.*, Phys. Rep. **42**, 14 (2006).
[12] B. B. Back *et al.*, Rev. Mod. Phys. **86**, 317 (2014).
[13] M. S. Gautam, Can. J. Phys. **93**, 1343 (2015).
[14] M. S. Gautam, Chin. Phys. C **39**, 114102 (2015).
[15] L. T. Baby *et al.*, Phys. Rev. C **62**, 014603 (2000).
[16] A. A. Sonzogni *et al.*, Phys. Rev. C **57**, 722 (1998).
[17] M. S. Gautam, Rajni, and M. K. Sharma, Braz. J. Phys. **46**, 133 (2016).
[18] M. S. Gautam *et al.*, Phys. Rev. C **92**, 054605 (2015).
[19] M. S. Gautam, Mod. Phys. Lett. A **30**, 1550013 (2015).
[20] J. D. Bierman *et al.*, Phys. Rev. Lett. **76**, 1587 (1996).
[21] A M Stefanini *et al.*, Phys. Lett. B **728**, 639 (2014).
[22] M. S. Gautam, Acta. Phys. Pol. B **46**, 1055 (2015.
[23] M. S. Gautam, Nucl. Phys. A **933**, 272 (2015).
[24] H. Esbensen, Phys. Rev. C **68**, 034604 (2003).
[25] H. Esbensen, Phys. Rev. C **72**, 054607 (2005).
[26] Z. F. Muhammad *et al.*, Phys. Rev. C **81**, 044609 (2010).
[27] T. Rumin, K. Hagino, and N. Takigawa, Phys. Rev. C **61**, 014605 (1999).
[28] M. S. Gautam, Int. J. Mod. Phys. E **26**, 1750063 (2017).
[29] M. S. Gautam, Commun. Theor. Phys. **64**, 710 (2015).
[30] M. S. Gautam, Indian J. Phys. **90**, 335 (2016).
[31] R. G. Stokstad *et al.*, Phys. Rev. C **23**, 281 (1981).
[32] E. F. Aguilera *et al.*, Phys. Rev. C **41**, 910 (1990).
[33] E. F. Aguilera *et al.*, Phys. Rev. C **52**, 3103 (1995).
[34] E. M. Quiroz *et al.*, Phys. Rev. C **63**, 054611 (2001).
[35] M. S. Gautam and M. K. Sharma, in *Advanced Materials and Radiation Physics (AMRP-2015): 4th National Conference on Advanced Materials and Radiation Physics*, edited by M. M. Sinha and S. S. Verma, AIP Conf. Proc. No. 1675 (AIP, New York, 2015), p. 020052.
[36] M. S. Gautam *et al.*, Braz. J. Phys. **47**, 461 (2017).
[37] M. S. Gautam, Chin. J. Phys. **54**, 86 (2016).
[38] C. Beck, J. Phy.: Conf. Ser. **420**, 012067 (2013).
[39] H. Timmers *et al.*, Phys. Lett. B **399**, 35 (1997).
[40] A. M. Stefanini *et al.*, Phys. Rev. C **73**, 034606 (2006).
[41] A. M. Stefanini *et al.*, Phys. Rev. C **76**, 014610 (2007).
[42] H. Q. Zhang *et al.*, Phys. Rev. C **82**, 054609 (2010).
[43] M. S. Gautam, Chin. Phys. C **40**, 054101 (2016).
[44] F. Scarlassara *et al.*, Prog. Theor. Phys. Suppl. **154**, 31 (2004).
[45] M. Beckerman *et al.*, Phys. Rev. Lett. **45**, 1472 (1980).
[46] M. S. Gautam, K. Vinod, and H. Kumar, Chinese J. Phys. **54**, 515 (2016).
[47] V. Tripathi *et al.*, Phys. Rev. C **65**, 014614 (2001).
[48] M. Trotta *et al.*, Phys. Rev. C **65**, 011601(R) (2001).
[49] M. S. Gautam, Braz. J. Phys. **46**, 143 (2016).
[50] P. H. Stelson *et al.*, Phys. Rev. C **41**, 1584 (1990).
[51] Y. Yu. Denisov, Eur. Phys. J. A **7**, 87 (2000).
[52] V. I. Zagrebaev, Phys. Rev. C **67**, 061601(R) (2003).
[53] V. V. Sargsyan *et al.*, Phys. Rev. C **84**, 064614 (2011).
[54] V. V. Sargsyan *et al.*, Eur. Phys. J. A **49**, 54 (2013).
[55] G. L. Zhang, X. X. Liu, and C. J. Lin, Phys. Rev. C **89**, 054602 (2014).
[56] A. B. Balantekin and N. Takigawa, Rev. Mod. Phys. **70**, 77 (1998).
[57] K. Hagino and N. Takigawa, Prog. Theor. Phys. **128**, 1061 (2012).
[58] L. F. Canto, P. R. S. Gomes, R. Donangelo, J. Lubian, and M. S. Hussein, Phys. Rep. **596**, 1 (2015).
[59] J. O. Newton *et al.*, Phys. Rev. C **64**, 064608 (2001).
[60] S. Kalkal *et al.*, Phys. Rev. C **81**, 044610 (2010).
[61] S. Kalkal *et al.*, Phys. Rev. C **83**, 054607 (2011).
[62] S. Kalkal *et al.*, Phys. Rev. C **85**, 034606 (2012).
[63] Khushboo *et al.*, Phys. Rev. C **96**, 014614 (2017).
[64] K. Hagino, N. Rowley, and A. T. Kruppa, Comput. Phys. Commun. **123**, 143 (1999).
[65] M. Singh, Sukhvinder, and R. Kharab, Mod. Phys. Lett. A **26**, 2129 (2011).
[66] M. Singh, Sukhvinder, and R. Kharab, Nucl. Phys. A **897**, 179 (2013).
[67] M. Singh, Sukhvinder, and R. Kharab, Nucl. Phys. A **897**, 198 (2013).
[68] M. S. Gautam, Phys. Rev. C **90**, 024620 (2014).
[69] M. S. Gautam *et al.*, Eur. Phys. J. A **53**, 12 (2017).
[70] M. S. Gautam *et al.*, Eur. Phys. J. A **53**, 212 (2017).
[71] M. S. Gautam, Int. J. Mod. Phys. E **28**, 1950006 (2019).
[72] M. S. Gautam, H. Khatri, and K. Vinod, Nucl. Phys. A **984**, 9 (2019).
[73] M. S. Gautam, K. Vinod, S. Duhan, R. P. Chahal, and H. Khatri, Nucl. Phys. A **998**, 121730 (2020).
[74] D. L. Hill and J. A. Wheeler, Phys. Rev. **89**, 1102 (1953).
[75] C. Y. Wong, Phys. Rev. Lett. **31**, 766 (1973).
[76] J. O. Newton *et al.*, Phys. Rev. C **70**, 024605 (2004).
[77] A. Mukherjee *et al.*, Phys. Rev. C **75**, 044608 (2007).
[78] L. C. Chamon *et al.*, Phys. Rev. C **66**, 014610 (2002).
[79] L. C. Chamon *et al.*, Phys. Rev. Lett. **79**, 5218 (1997).
[80] M. A. C. Ribeiro *et al.*, Phys. Rev. Lett. **78**, 3270 (1997).
[81] C. Simenel *et al.*, Phys. Rev. C **88**, 064604 (2013).
[82] C. Simenel, Eur. Phys. J. A **48**, 152 (2012).
[83] K. Washiyama and D. Lacroix, Phys. Rev. C **78**, 024610 (2008).
[84] A. S. Umar, C. Simenel, and V. E. Oberacker, Phys. Rev. C **89**, 034611 (2011).
[85] A. S. Umar and V. E. Oberacker, Eur. Phys. J. A **39**, 243 (2009).
[86] E. F. Aguilera and J. J. Kolata, Phys. Rev. C **85**, 014603 (2012).
[87] K. Hagino *et al.*, J. Phys. G **23**, 1413 (1997).
[88] K. Hagino *et al.*, Phys. Rev. C **57**, 1349 (1998).

[89] Z. F. Muhammad *et al.*, Phys. Rev. C **77**, 014606 (2008).
[90] W. Henning *et al.*, Phys. Rev. C **17**, 2245 (1978).
[91] K. Washiyama, K. Hagino, and M. Dasgupta, Phys. Rev. C **73**, 034607 (2006).
[92] K. Hagino, T. Takehi, A. B. Balantekin, and N. Takigawa, Phys. Rev. C **71**, 044612 (2005).
[93] N. Wang *et al.*, Phys. Rev. C **65**, 064608 (2002).
[94] N. Wang *et al.*, Phys. Rev. C **67**, 024604 (2003).
[95] A. Iwamoto and K. Harada, Z. Phys. A **326**, 201 (1987).
[96] V. N. Kodratyev *et al.*, Phys. Rev. C **61**, 044613 (2000).
[97] H. M. Jia *et al.*, Phys. Rev. C **89**, 064605 (2014).
[98] M. V. Chushnyakova and I. I. Gontchar, Phys. Rev. C **87**, 014614 (2013).
[99] M. V. Chushnyakova, R. Bhattacharya, and I. I. Gontchar, Phys. Rev. C **90**, 017603 (2014).
[100] I. I. Gontchar, R. Bhattacharya, and M. V. Chushnyakova, Phys. Rev. C **89**, 034601 (2014).